CARTILAGE
2025, Vol. 16(2) 190–201
© The Author(s) 2023
DOI: 10.1177/19476035231200359
journals.sagepub.com/home/CAR
Sage

Heterogeneous Characteristics of the CD90$^+$ Progenitors in the Fibrocartilage of Different Joints

Yiru Wang[1], Qianli Li[1], Haohan Li[1], Xianni Yang[1], Han Fang[1], Ruiye Bi[1], and Songsong Zhu[1]

Abstract

Objective. This study aimed to isolate and compare the mesenchymal stem cell characteristics of CD90$^+$ cells from different fibrocartilage tissues in the temporomandibular joint (TMJ), the knee joint, and the intervertebral joint to further understand the similarities and differences of these 4 fibrocartilage tissues. *Methods.* CD90$^+$ cells were isolated from TMJ disc, condylar cartilage, meniscus, and intervertebral disc by using magnetic-activated cell sorting. Cellular assays including 4.5-ethynyl-2′-deoxyuridine labeling, multilineage differentiation, colony formation, and cell migration were conducted to compare their mesenchymal stem cell characteristics. Immunofluorescent staining was performed for observing the expression of actively proliferating CD90$^+$ cells within the tissues. H&E staining and Safranine O staining were used to compare the histological features. *Results.* The CD90$^+$ cells derived from these 4 fibrocartilage tissues exhibited comparable cell proliferation abilities. However, the cells from the TMJ disc displayed limited multilineage differentiation potential, colony formation, and cell migration abilities in comparison with the cells from the other fibrocartilage tissues. *In vivo*, there was relatively more abundant expression of CD90$^+$ cells in the TMJ disc during the early postnatal stage. The limited EDU$^+$ cell numbers signified a low proliferation capacity of CD90$^+$ cells in the TMJ disc. In addition, we observed a significant decrease in cell density and a restriction in the synthesis of extracellular proteoglycans in the TMJ disc. *Conclusion.* Our study highlights the spatial heterogeneity of CD90$^+$ cells in the fibrocartilages of different joint tissues, which may contribute to the limited cartilage repair capacity in the TMJ disc.

Keywords

progenitor cell, fibrocartilage, temporomandibular joint disc

Introduction

Fibrocartilage is a common tissue type that is found in various anatomical locations, including the intervertebral disc (IVD), meniscus, temporomandibular joint (TMJ) disc, condylar cartilage, and tendon-bone junctions. Unlike hyaline cartilage, fibrocartilage is composed of both cartilaginous and fibrous tissue, and is considered a transitional tissue between hyaline cartilage and dense regular connective tissues, such as tendons and ligaments.[1] In addition, fibrocartilage contains high levels of type I collagen, along with type II collagen and a small amount of ground substance.[1] Its primary function is mechanical, and it is able to withstand both compressive and tensile forces. Disruption of homeostasis in articular cartilage can occur due to injury or with increasing age. Post-injury fibrocartilage repair continues to be a challenge. Due to the lack of vascularization,

[1]State Key Laboratory of Oral Diseases & National Center for Stomatology & National Clinical Research Center for Oral Diseases, Department of Orthognathic and Temporomandibular Joint Surgery, West China Hospital of Stomatology, Sichuan University, Chengdu, China

Corresponding Authors:

Songsong Zhu, State Key Laboratory of Oral Diseases & National Center for Stomatology & National Clinical Research Center for Oral Diseases, Department of Orthognathic and Temporomandibular Joint Surgery, West China Hospital of Stomatology, Sichuan University, No. 14, 3rd Section of Ren Min Nan Road, Chengdu 610041, Sichuan, China.
Email: zss_1977@163.com

Ruiye Bi, State Key Laboratory of Oral Diseases & National Center for Stomatology & National Clinical Research Center for Oral Diseases, Department of Orthognathic and Temporomandibular Joint Surgery, West China Hospital of Stomatology, Sichuan University, No. 14, 3rd Section of Ren Min Nan Road, Chengdu 610041, Sichuan, China.
Email: david-bry@foxmail.com

low chondrocyte density, and high matrix-to-cell ratio, cartilage has limited regenerative capabilities after injury.[2] Moreover, since cartilage is aneural, symptoms usually appear only after significant structural destruction of the matrix.[3] As a result, damage and degeneration of fibrocartilage, which can include meniscus injuries, temporomandibular joint disorders (TMDs), and intervertebral disc degeneration (IDD), can lead to severe tissue loss and disability, thus significantly affecting the productivity and quality of life of patients ranging from children to the elderly.

Interestingly, the prevalence of fibrocartilage damage and degeneration varies across age groups. TMD has a higher prevalence in young and middle-aged adults, with the peak occurrence being between 20 and 40 years of age.[4] The most prevalent TMD condition is displacement of the TMJ anterior disc displacements with reduction, followed by degenerative joint disease.[5] In comparison, meniscus injuries are more commonly observed in younger populations with physically demanding occupations, as well as in older populations.[6,7] IDD has been identified in childhood, but its prevalence increases with age, with the highest rate found in the elderly.[8-10] These differences in age-specific prevalence suggest that there is a heterogeneity among the fibrocartilage tissues and that the peak ages for the prevalence of TMD are earlier than those for meniscus injuries and IDD. It is generally believed that injuries are better repaired at a younger age because these patients have more progenitor cells. However, the peak prevalence of TMD was observed in young and middle-aged populations. The potential underlying reasons for this phenomenon are complex and may include factors such as orthodontic misalignment,[11] oral habit activities (e.g., gum chewing, pen biting),[12] and psychological factors.[13] Nonetheless, the present findings suggest that repair after a TMJ injury remains challenging.[14]

Stem/progenitor cells have been identified as the most suitable cell type for repair after cartilage injuries due to their availability and the lack of donor morbidities.[15] Several studies have shown that populations of stem/progenitor cells reside in fibrocartilage.[16-18] One classical marker of mesenchymal stromal cells (MSCs) in fibrocartilage is cluster of differentiation 90 (CD90). CD90 has been implicated in MSCs' ability to interact with the extracellular matrix (ECM), modulate immune responses, and promote tissue regeneration; in addition, it is involved in various cellular processes, including cell adhesion, migration, proliferation, and signaling.[19] Based on the $CD90^+$ cells in fibrocartilage from previous research,[20-22] our study isolated the stem/progenitor cells ($CD90^+$ cells) from the fibrocartilages in the mouse TMJ disc, condylar cartilage, meniscus, and IVD to compare similarities and differences, aiming to enhance the understanding of these tissues in clinical prognoses and research.

Materials and Methods

The study was performed in accordance with the recommendations from the Guide for the Care and Use of Laboratory Animals of Sichuan University. The animal procedures were performed according to protocols that were approved by the Animal Ethics Committee of Sichuan University (WCHSIRB-D-2020-476) and followed the guidelines of Animal Research: Reporting of In Vivo Experiments.

Animals

C57BL/6 wild-type mice were purchased from ENSIWEIER (Chengdu, China) and housed in individually ventilated cages (5 mice/cage) under pathogen-free conditions in a temperature-controlled facility (22 ± 1°C, 12-hour light/dark cycle) with free access to standard food and water. The TMJ disc, condylar cartilage, meniscus, and IVD were all harvested from the same animal and collected at the same time. All the male/female mice were wild-type mice selected from different litters randomly. Three-day-old to 1-week-old mice were both male and female. Three-week-old, 8-week-old, and 26-week-old mice used for the experiments were males to avoid the potential impact of estrogen on bone. All the mice were anesthetized by isoflurane before sacrificed.

Cell Isolation and Culture

$CD90^+$ cells were isolated from newborn mice (3-day-old to 1-week-old), as stem/progenitor cells are more abundant in fetal and young tissues. $CD90^+$ cells were obtained via a magnetically activated cell sorting (MACS) method and then cultured *in vitro* (**Fig. 1A** and **B**). First, all the tissues were dissected into 1 × 1 mm^2 pieces and immediately placed in phosphate-buffered saline (PBS) solution. Then, the tissues were digested in 4 mg/ml pronase (10165921001; Roche, Switzerland) for 1 hour and 2 mg/ml collagenase P (11213857001; Roche, Switzerland) for 1 hour at 37°C with shaking. All the pronase and collagenase were from the same batch. After filtering to remove tissue debris, the cells were harvested and resuspended in a MACS buffer (PBS supplemented with 0.5% bovine serum albumin [BSA] and 2 mM ethylenediaminetetraacetic acid [EDTA]). MACS was performed with CD90.2 microbeads (130-121-278; Miltenyi Biotec, Germany) to isolate the $CD90^+$ stem/progenitor cells. The $CD90^+$ cells were cultured in complete alpha Dulbecco's Modified Eagle Medium (αMEM) (C12571500BT; Gibco, USA) with 20% fetal bovine serum (FBS) (10091148; Gibco, USA) and 1% penicillin/streptomycin (15140122; Gibco, USA) at 37°C in a humidified incubator containing 5% CO_2. The medium was exchanged

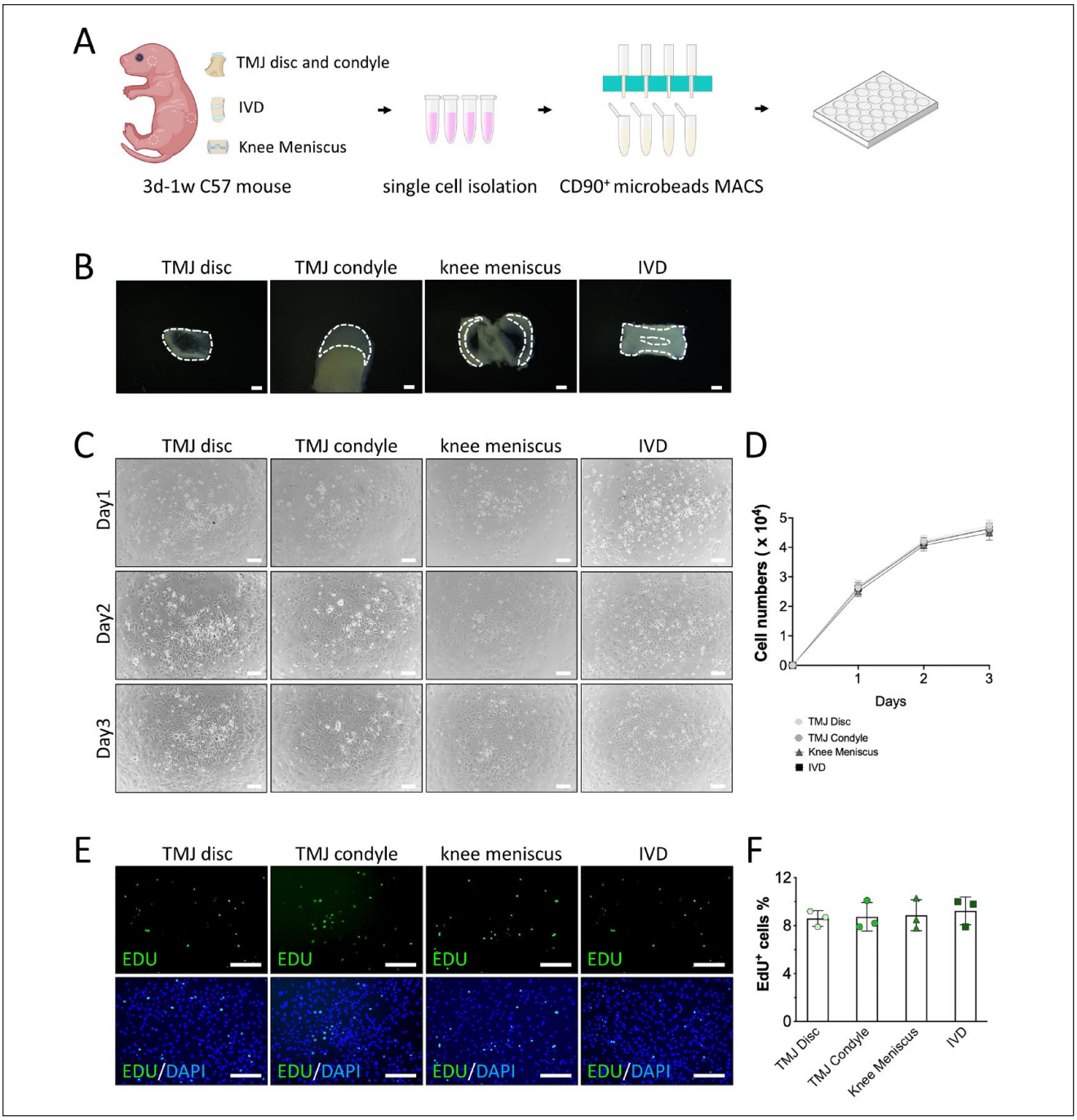

Figure 1. Growth and proliferation of CD90$^+$ cells from the TMJ disc, condylar cartilage, meniscus, and IVD *in vivo*. (**A**) The workflow of the CD90$^+$ cell retrieval strategy. (**B**) The TMJ disc, condylar cartilage, meniscus, and IVD were harvested from 3-day-old to 1-week-old mice. Scale bar = 200 μm. (**C**) CD90$^+$ cells that were observed under light microscopy on day 1, day 2, and day 3. Scale bar = 200 μm. (**D**) Cell growth curve of the CD90$^+$ cells. *N* = 6 biological replicates. Data are presented as the mean ± SD. A 2-way ANOVA with Tukey's multiple comparison test was used for the data analysis. (**E**) Cell proliferation according to EdU staining. EdU: slow-cycling cells (green). DAPI: cell nuclei (blue). Scale bar = 250 μm. (**F**) Quantification of the EdU+ cells% (mean ± SD) in CD90$^+$ cells. *N* = 3 biological replicates. A 1-way ANOVA was used for the analysis. CD90 = cluster of differentiation 90; TMJ = temporomandibular joint; IVD = intervertebral disc; SD = standard deviation; ANOVA = analysis of variance; EdU = 4.5-ethynyl-2′-deoxyuridine.

completely every 3 days. When the cultures reached 75% confluence, the cells were subcultured using 0.25% trypsin-EDTA (25200072; Gibco, USA).

4.5-Ethynyl-2′-Deoxyuridine Labeling

C0071 BeyoClickTM 4.5-ethynyl-2′-deoxyuridine (EdU)-488 was used to measure the proliferation capacity of the cells in *in vitro* experiments. When the $CD90^+$ cells reached 50% confluence, 10 μM EdU was added to the culture medium and incubated for 4 hours. The cells were then fixed with 4% paraformaldehyde (PFA) and incubated with Click Additive Solution. The nuclei were counterstained with 4′,6-diamidino-2-phenylindole (DAPI) (C0065; Solarbio, China).

For analysis of cell proliferation, 7-day-old mice were weighed and injected with 30 μg/g EdU (A10044; Invitrogen, USA) 24 hours prior to the time of sacrifice. EdU^+ cells were detected with the Cell-LightTM EdU Apollo 488 In Vitro Kit (C10310-3; Ribobio, China) according to the manufacturer's protocol. EdU^+ cells were visualized and counted under a fluorescence microscope (DMi8; Leica, Germany).

Multilineage Differentiation Assay

For osteogenesis, when $CD90^+$ cells had reached 60% to 70% confluence, osteogenesis differentiation medium was added. This medium contained αMEM supplemented with 10% FBS, 10^{-8} mol dexamethasone (D8040; Solarbio, China), 50 μg/m L-ascorbic acid (231406; J&K Scientific, China), and 10 mM β-glycerophosphate (G8100; Solarbio, China). After induction of osteogenesis for 3 weeks, the cells were fixed with 4% PFA and stained with 1% Alizarin red (G1452; Solarbio, China).

For chondrogenesis, $CD90^+$ cells were pelleted in V-bottom 96-well plates (2.5×10^5 cells/well) via centrifugation and cultured for 3 weeks. The chondrogenesis medium was the same as that described in a previous study.[23] The pellets were fixed with 4% PFA and prepared for either paraffin or frozen embedded sections. Safranin O/fast green staining (G1371; Solarbio, China) was then performed.

For adipogenic differentiation, adipogenesis-inducing media A and B were used, as described in a previous study.[23] When the $CD90^+$ cells had reached 80% to 90% confluence, medium A was added and cultured for 2 days, then replaced with medium B for 6 days. Lipid droplets were visualized under a light microscope and analyzed via Oil Red O staining.

Colony Formation Assay

$CD90^+$ cells were harvested in the logarithmic phase and cultured in 6-well plates (800 cells per well). After culturing for 12 days, the cells were fixed with 4% PFA and stained with 0.1% crystal violet dye.

Cell Migration Assay

To analyze the cell migration, 2×10^4 cells, in serum-free medium, were seeded into the upper chamber. A medium containing 20% FBS was added to the lower chamber to serve as a chemoattractant. After 48 hours of incubation, the upper chamber was removed and washed with PBS. The cells were then fixed with PFA and stained with 0.1% crystal violet. The cells in the upper chamber that did not migrate were gently wiped off with a cotton swab, and the number of cells that migrated were counted under a microscope.

Flow Cytometry

Tissues were isolated from 3-day-old to 1-week-old C57BL/6 mice and cut into small pieces. Next, the pieces were digested with pronase for 1 hour and collagenase P for 1 hour, as previously described. For the flow cytometric analysis, the cells were immunolabeled with 3.5 μl of CD90.2 fluorescent conjugated antibodies (105316; Biolegend, USA) or isotype-matched IgG controls (400625; Biolegend, USA) for 30 minutes on ice. Flow cytometry (FCM) was performed using a flow cytometer (AttuneTM NxT Flow Cytometer; Thermo Fisher Scientific, USA). The sample gating strategies for all FCM experiments are shown in **Figure 3A**.

Histology

Tissue samples were fixed in 4% PFA, decalcified in EDTA, and prepared for either paraffin or frozen embedded sections. Tissue sections were stained with hematoxylin and eosin (BL700A; Biosharp, China) and Safranin O/fast green staining.

Immunofluorescence Staining

Cryosections were immunofluorescence-stained following standard protocols. Permeabilization was performed with 0.5% Triton in PBS. The samples were blocked with 5% goat serum in 3% BSA in PBS for 1 hour at room temperature. CD90.2 (14-0902-82; Invitrogen, 1:100, USA) was incubated at 4°C overnight. Goat anti-rat Alexa fluor 488 (a23240; Abbkine, 1:500, USA) was incubated for 1 hour. DAPI was used for counterstaining.

Statistical Analysis

Each experiment contained at least 3 independent biorepeats. Results were given as means and standard deviations (SDs). Two blinded and independent observers performed

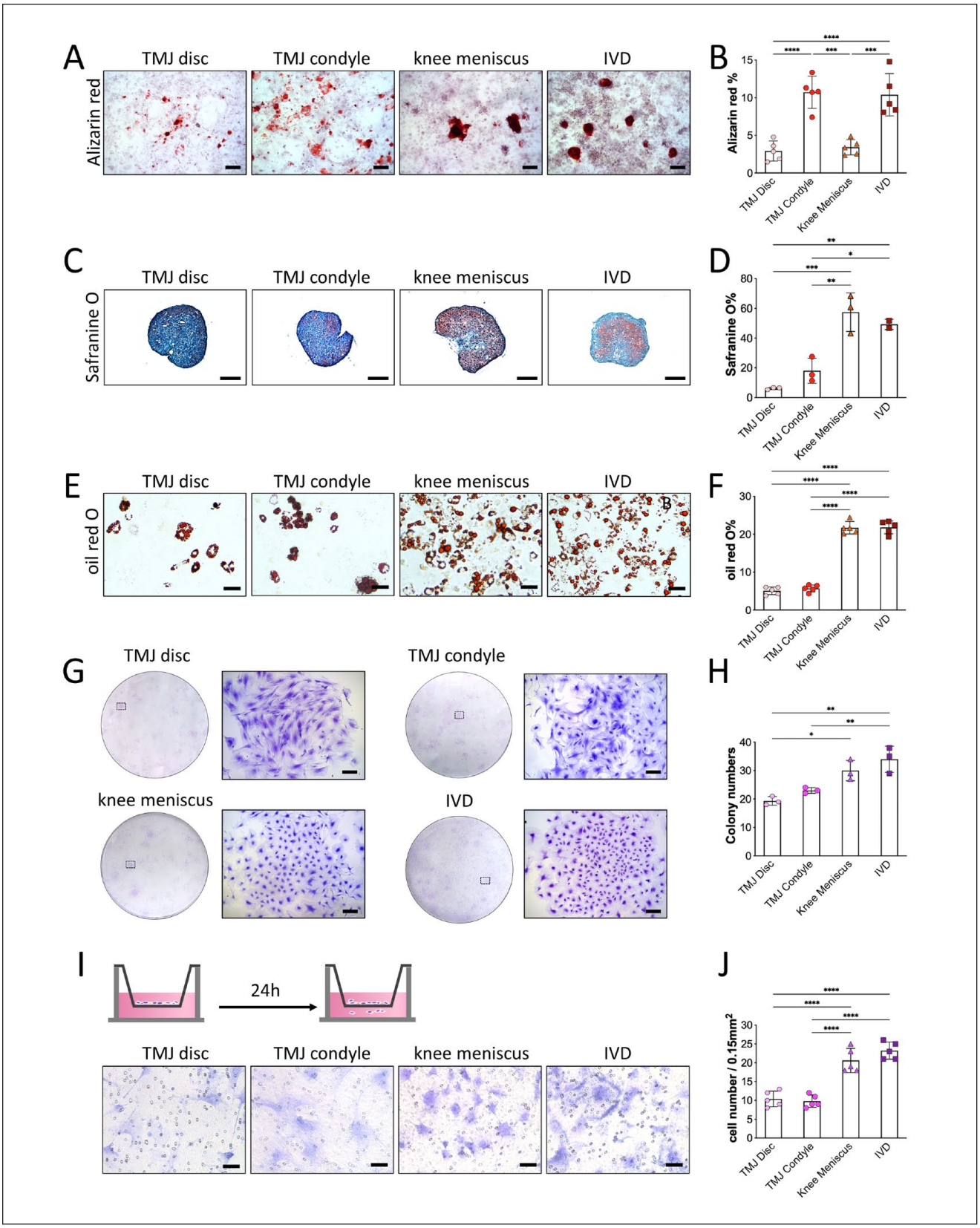

Figure 2. CD90$^+$ cells exhibited distinct progenitor characteristics from the fibrocartilage of different joints. Multipotential differentiation *in vitro* (**A-F**). (**A**) Alizarin Red staining demonstrating calcium deposition in osteogenic media. Scale bar = 250 μm. (**B**) The percentage of the Alizarin Red+ area was quantified with ImageJ. Data are presented as the mean values ± SD. *N* = 5

(continued)

Figure 2. (continued)

biological replicates. Significance was assessed with 1-way ANOVA. *** (Knee meniscus vs. TMJ condyle) $P = 0.0001$, *** (knee meniscus vs. IVD) $P = 0.0002$, ****$P < 0.0001$. (**C**) Safranin O immunostaining showing the chondrogenic potential in pellet cultures. Scale bar = 250 μm. (**D**) The percentage of the Safranin O+ area was quantified with ImageJ. Data are presented as the mean values ± SD. $N = 3$ biological replicates. Significance assessed with 1-way ANOVA. *** (TMJ disc vs. knee meniscus) $P = 0.0006$, **(TMJ disc vs. IVD) $P = 0.0033$, ** (knee meniscus vs. TMJ condyle) $P = 0.0029$, *(TMJ condyle vs. IVD) $P = 0.0188$. (**E**) Oil red O staining in lipid droplets in adipogenic media. Scale bar = 50 μm. **(F)** The percentage of the Oil red O + area was quantified with ImageJ. Data are presented as the mean values ± SD. $N = 5$ biological replicates. Significance was assessed with 1-way ANOVA. ****$P < 0.0001$. (**G**) Clonogenicity according to the colony-forming assay. Scale bar = 250 μm. (**H**) Numbers of colonies quantified with ImageJ. Data are presented as the mean values ± SD. $N = 3$ biological replicates. Significance was assessed with 1-way ANOVA. * (TMJ disc vs. knee meniscus) $P = 0.0115$, **(TMJ disc vs. IVD) $P = 0.0017$, ** (TMJ condyle vs. IVD) $P = 0.0097$. (**I**) Schematic illustration of the different parts of the Transwell system (top). Micrographs of the $CD90^+$ cells in different groups at the bottom of the Transwell culture migration chamber. Scale bar = 50 μm. (**J**) The cell numbers of the migrated cells were quantified with ImageJ. Data are presented as the mean values ± SD. $N = 5$ biological replicates. Significance was assessed with 1-way ANOVA. CD90 = cluster of differentiation 90; SD = standard deviation; ANOVA = analysis of variance; TMJ = temporomandibular joint; IVD = intervertebral disc. ****$P < 0.0001$.

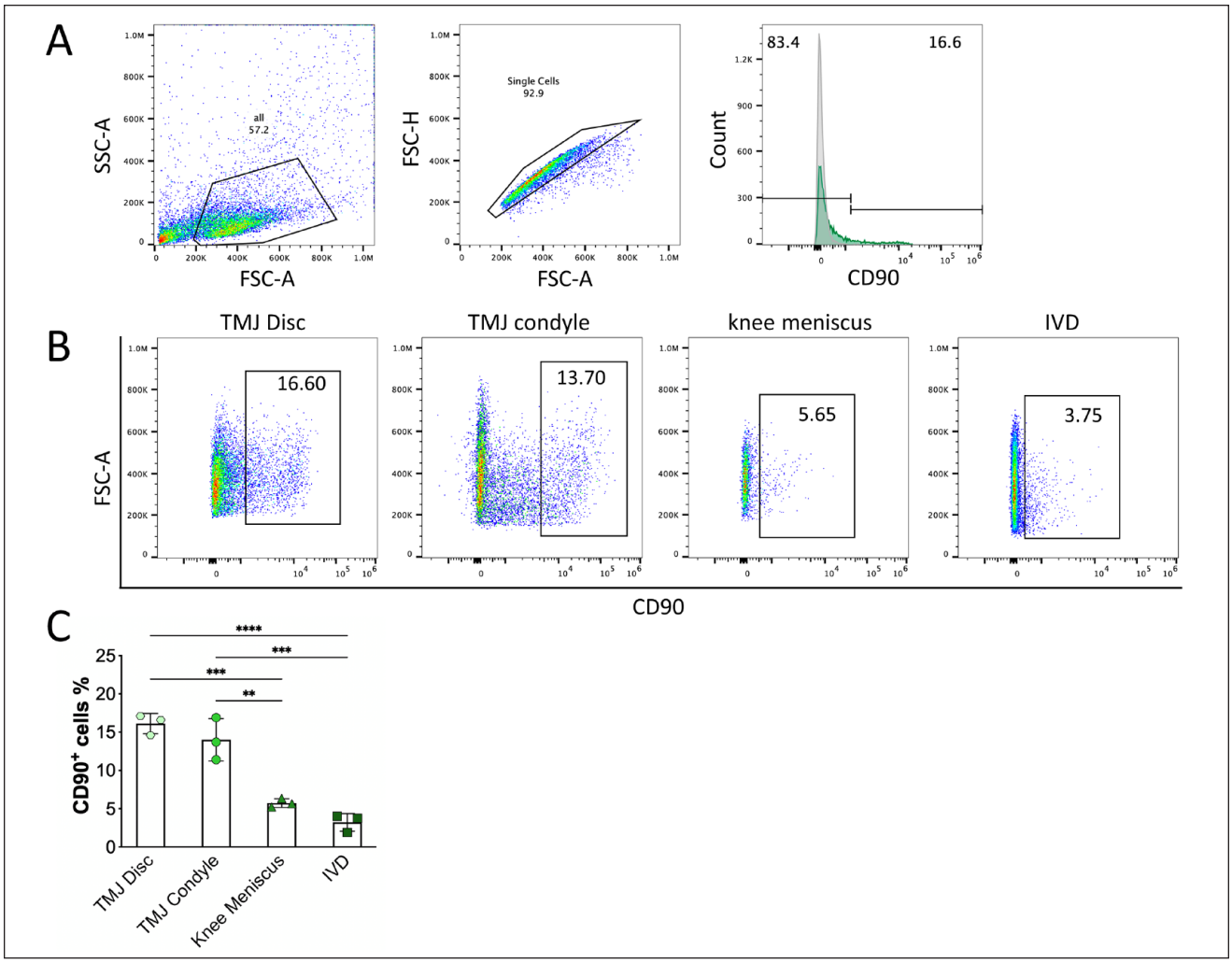

Figure 3. The proportion of CD90+ progenitors in the fibrocartilage of different joints *in vivo*. (**A**) Gating strategies in flow cytometry. The forward scatter (FSC) versus side scatter (SSC) gating strategy was used to exclude cell debris and dead cells, which tended to have lower forward-scatter levels and are found at the bottom-left corner of the FSC versus SSC density plot. Apoptotic cells tended to have a lower FSC and higher SSC. The FCS-A versus FSC-H gating strategy was used to exclude doublets and to screen out single cells. Each test had a blank control that was used to screen out positive cells. (**B**) Flow cytometric plot of $CD90^+$ cells in different fibrocartilages. (**C**) The percentage of $CD90^+$ cells (mean ± SD). $N = 3$ biological replicates. A 1-way ANOVA with Tukey's multiple comparison test was used for the analysis. CD90 = cluster of differentiation 90; SD = standard deviation; ANOVA = analysis of variance; TMJ = temporomandibular joint; IVD = intervertebral disc. *** (TMJ disc vs. knee meniscus) $P = 0.0003$, ** (knee meniscus vs. TMJ condyle) $P = 0.0013$, *** (TMJ condyle vs. IVD) $P = 0.0002$, ****$P < 0.0001$.

the measurements. The staining results were analyzed with ImageJ software version 1.51 (Leeds Precision Instruments). The results of the FCM analyses were analyzed using FlowJo (version 10.6.2; Tree Star, USA). All statistical analyses were calculated using Prism 9 (GraphPad Software). The statistical significance of the differences among the 4 groups was determined by using 1-way analysis of variance (ANOVA) with Tukey's multiple comparisons. The statistical differences in the cell density (**Fig. 5B**) and Safranine O^+ area (**Fig. 5D**) at different ages and in the cell growth curves (**Fig. 1D**) were determined by using 2-way ANOVA with Tukey's multiple comparisons. Differences were considered statistically significant when the P value was <0.05.

Results

Growth and Proliferation of CD90$^+$ Cells from the TMJ Disc, Condylar Cartilage, Meniscus, and IVD In Vitro

The proliferation rates of the $CD90^+$ cells at P3 were evaluated on day 1, day 2, and day 3. The growth curves of the $CD90^+$ cells from the 4 fibrocartilage tissues showed similar trends, with rapid proliferation in the first 2 days, followed by slower proliferation on day 3 (**Fig. 1C** and **D**). However, differences in cell morphology were observed during proliferation, with $CD90^+$ cells from the TMJ disc and condylar cartilage, exhibiting a more "fibroblast-like" spindle shape, while $CD90^+$ cells from the meniscus and IVD displayed a more rounded and "chondrocyte-like" shape (**Fig. 1C**).

At the same time, the EdU staining showed that there were no significant differences in the proliferation capacity of the $CD90^+$ cells from the 4 fibrocartilage tissues (**Fig. 1E** and **F**). Our findings indicate that the $CD90^+$ cells from all 4 fibrocartilage tissues exhibited comparable cell proliferation abilities.

CD90$^+$ Cells from the TMJ Disc had the Weakest Multilineage Differentiation Potential, Colony Formation Capacity, and Migration Abilities

To investigate the differentiation potential of the $CD90^+$ cells from different fibrocartilages, we subjected them to osteogenic, chondrogenic, and adipogenic differentiation. The osteogenic differentiation was assessed according to the formation of calcified deposits that were stained with Alizarin Red. The $CD90^+$ cells from TMJ disc and meniscus exhibited significantly reduced osteogenic differentiation capacities compared to the condylar cartilage and IVD (**Fig. 2A** and **B**). Chondrogenic differentiation was verified according to the formation of Safranin O^+ proteoglycan. The chondrogenic pellets from the TMJ disc and condylar cartilage had only limited Safranin O^+ cells, while the pellets from the meniscus and IVD had abundant proteoglycan$^+$ content (**Fig. 2C** and **D**). The adipogenic differentiation was evaluated according to the formation of Oil Red O^+ lipid droplets. Only small amounts of Oil-Red-O-stained granules were detected in the TMJ disc and condylar cartilage, whereas they were distinctly observed in the meniscus and IVD (**Fig. 2E** and **F**).

The colony formation assay demonstrated that the number of colonies of $CD90^+$ cells from the TMJ disc and condylar cartilage had a more diffuse distribution and that fewer colonies were formed in comparison with the $CD90^+$ cells from the meniscus and IVD (**Fig. 2G** and **H**). Similar to the primary cell culture, the colonies from the TMJ disc and condylar cartilage displayed a morphology of elongated spindle-shaped cells, whereas the colonies from the meniscus and IVD displayed a rounded morphology (**Fig. 2G** and **H**).

Transwell assay showed that the $CD90^+$ cells from the TMJ disc and condylar cartilage had weaker migration than those from the meniscus and IVD (**Fig. 2I** and **J**).

These results supported that the $CD90^+$ cells from the TMJ disc had the most limited multilineage differentiation potential, colony formation ability, and cell migration capacity compared to the cells from the other fibrocartilage tissues from different joints.

Heterogeneity of CD90$^+$ Expression and Function in Different Fibrocartilages in the Joints of Postnatal Mice

Flow cytometric analysis indicated a significant increase in the number of $CD90^+$ cells in the TMJ disc and condylar cartilage compared to the meniscus and IVD (**Fig. 3B** and **C**).

Immunofluorescence staining showed the distribution of $CD90^+$ cells in the different joint fibrocartilages (**Fig. 4A** and **B**). The percentage of $CD90^+$ cells was found to be consistently significantly higher in the TMJ disc and condylar cartilage than in the other fibrocartilages. However, there were fewer EdU^+ cells in the TMJ disc than in the condylar cartilage (**Fig. 4C**). Co-staining showed that there were fewer $CD90^+$ cells with a proliferative status than were seen in the TMJ disc and the other fibrocartilages (**Fig. 4D**).

We further examined cell density in the different fibrocartilage tissues at different postnatal stages of mice. TMJ disc, condylar cartilage, meniscus, and IVD in 3-day-old, 3-week-old, 8-week-old, and 26-week-old mice were collected for H&E staining (**Fig. 5A**). Our analyses revealed that there were 2 distinct growth phases in all 4 fibrocartilage tissues, with the early postnatal stage (P3-P21) being characterized by a rapid increase in tissue size, shape, and cellularity with the later postnatal stage (P21-adulthood)

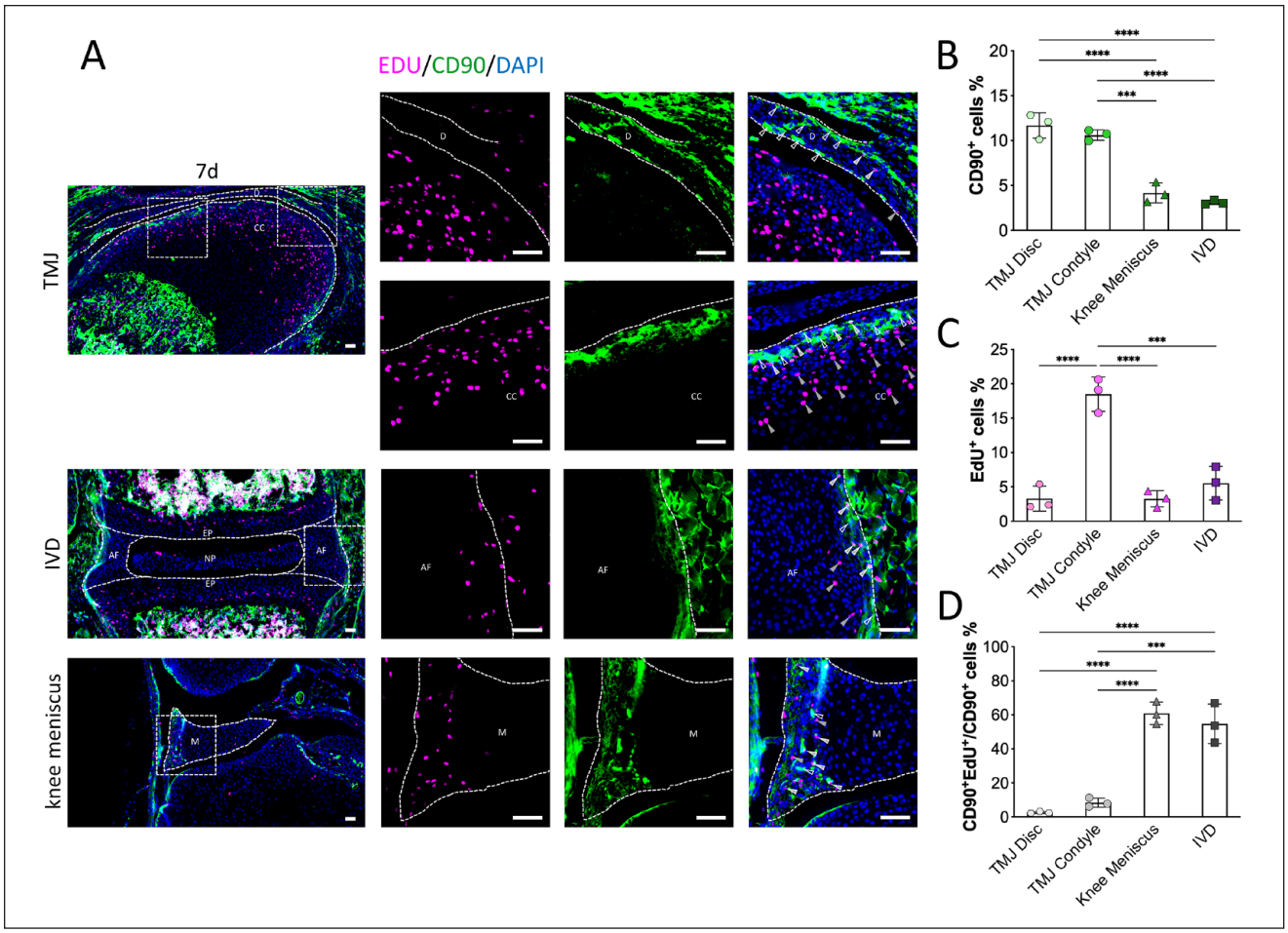

Figure 4. The distribution of CD90$^+$ progenitors in different joint fibrocartilages during early postnatal stages *in vivo*. (**A**) Immunofluorescence staining of TMJ discs during early postnatal stages for CD90 and EdU. Pink: EdU; Green: CD90; Blue: DAPI. D: TMJ disc, CC: condylar cartilage, EP: cartilaginous end plate, NP: nucleus pulposus, AF: annulus fibrosus, M: meniscus. White dotted lines: boundary of the tissue. Hollow arrow with white border: CD90$^+$ cells. Gray arrow: EdU+ cells. Gray arrow with white border: double-positive cells. Scale bar: 50 μm. (**B**) The numbers of CD90$^+$ cells from different fibrocartilages were quantified with ImageJ. Data are presented as the mean values ± SD. $N = 3$ independent animals. One-way ANOVA with Tukey's multiple comparison test was used for the data analysis. *** (Knee meniscus vs. TMJ condyle) $P = 0.0002$, ****$P < 0.0001$. (**C**) The numbers of EdU+ cells from different fibrocartilages were quantified with ImageJ. Data are presented as the mean values ± SD. $N = 3$ independent animals. One-way ANOVA with Tukey's multiple comparison test was used for the data analysis. *** (TMJ condyle vs. IVD) $P = 0.0003$, ****$P < 0.0001$. (**D**) The numbers of CD90$^+$ and EdU+ cells from different fibrocartilages were quantified with ImageJ. Data are presented as the mean values ± SD. $N = 3$ independent animals. One-way ANOVA with Tukey's multiple comparison test was used for the data analysis. CD90 = cluster of differentiation 90; TMJ = temporomandibular joint; EdU = 4.5-ethynyl-2′-deoxyuridine; DAPI = 6-diamidino-2-phenylindole; ANOVA = analysis of variance; SD = standard deviation; IVD = intervertebral disc.*** (TMJ condyle vs. IVD) $P = 0.0002$, ****$P < 0.0001$.

exhibiting only modest changes in these parameters. A sharp and statistically significant decrease in the cell density was observed in the TMJ disc (**Fig. 5B**). To evaluate the content and structure of the ECM during postnatal joint growth, Safranin O staining showed a significantly higher proteoglycan synthesis in the juvenile phase and a relatively lower proteoglycan synthesis in the aged phase in most of the fibrocartilage tissues, including the condylar cartilage, meniscus, and IVD (**Fig. 5C** and **D**). Interestingly, the TMJ disc was found to have little proteoglycan synthesis in all postnatal developmental stages that we observed.

Discussion

MSCs are thought to originate from pericytes and, therefore, to be in nearly all connective tissues, including fibrocartilage.[24] MSCs are typically defined by their adherence to plastic, trilineage differentiation capacity, self-renewal ability, and expression of specific cell surface markers.[25] CD90 is a common cell surface marker that is used to identify and characterize MSCs. CD90 has been shown to play a role in MSCs' adhesion, migration, and signaling.[19] Our study identified CD90$^+$ cells with mesenchymal stem cell

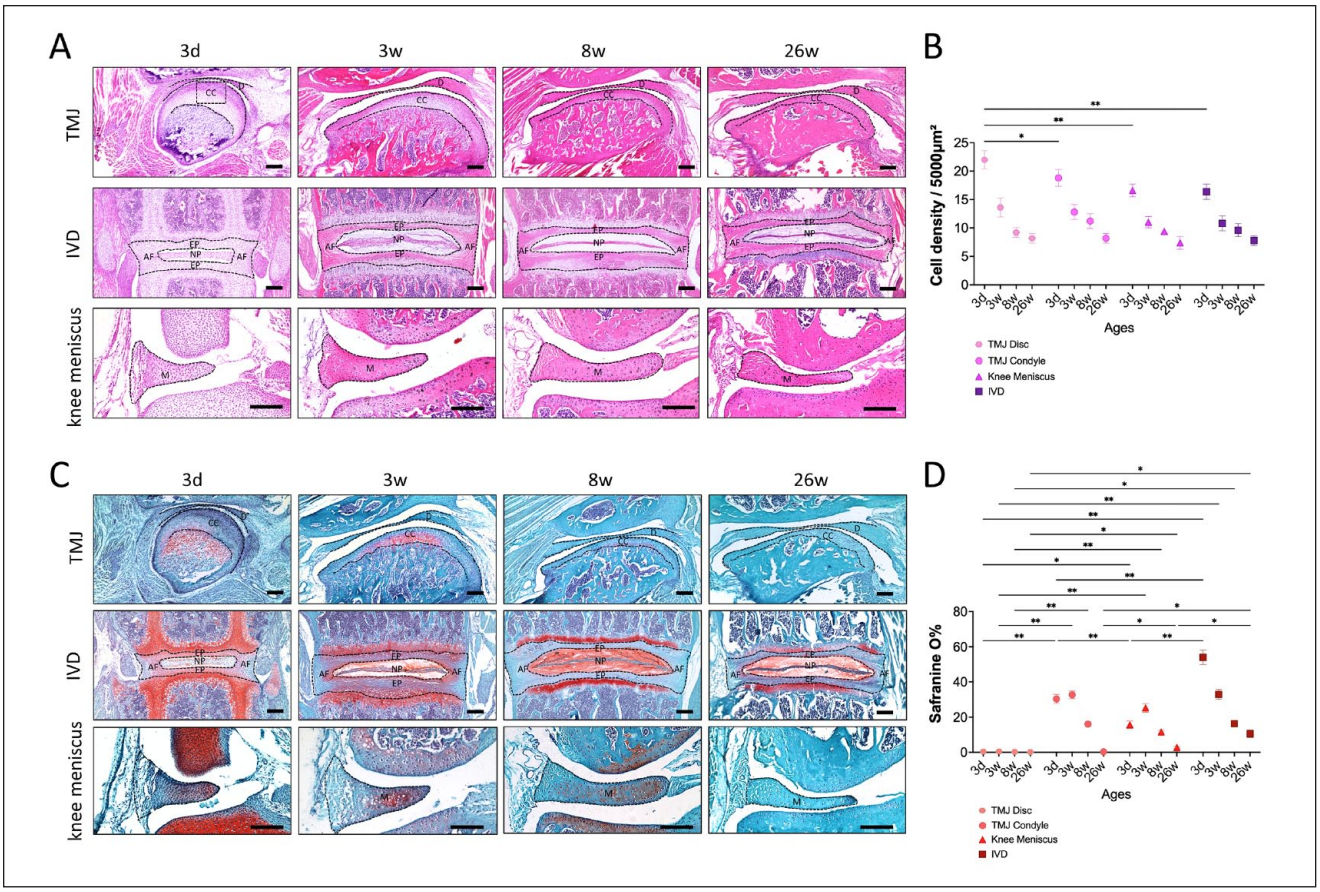

Figure 5. The cell density and ECM in different fibrocartilage tissues at different postnatal stages of mice. (**A**) H&E staining of fibrocartilage tissues in 3-day-old, 3-week-old, 8-week-old, and 26-week-old mice. Scale bar: 250 μm. D: TMJ disc, CC: condylar cartilage, EP: cartilaginous end plate, NP: nucleus pulposus, AF: annulus fibrosus, M: meniscus. Black dotted lines: boundary of the tissue. Scale bar: 250 μm. (**B**) Cell density (mean ± SD) of the fibrocartilage tissues at different stages. $N = 3$ independent animals. Two-way ANOVA with Tukey's multiple comparison test was used for the data analysis. * $P < 0.05$, ** $P < 0.01$, *** $P < 0.001$ and **** $P < 0.0001$. (**C**) Safranin O staining of in fibrocartilage tissues in 3-day-old, 3-week-old, 8-week-old, and 26-week-old mice. D: TMJ disc, CC: condylar cartilage, EP: cartilaginous end plate, NP: nucleus pulposus, AF: annulus fibrosus, M: meniscus. Black dotted lines: boundary of the tissue. Scale bar: 250 μm. (**D**) Semi-quantification of the Safranin O+ area (mean ± SD) in fibrocartilage tissues at different stages. $N = 3$ independent animals. Two-way ANOVA with Tukey's multiple comparison test was used for the data analysis. ECM = extracellular matrix; TMJ = temporomandibular joint; SD = standard deviation; ANOVA = analysis of variance; IVD = intervertebral disc. * $P < 0.05$, ** $P < 0.01$, *** $P < 0.001$, and **** $P < 0.0001$.

characteristics in various fibrocartilages, including the TMJ disc, condylar cartilage, meniscus, and IVD. The CD90$^+$ cells from the TMJ disc exhibited the lowest potential for chondrogenic, osteogenic, and adipogenic differentiation, while those from IVD showed the highest potential. Our findings suggest that CD90$^+$ cells may vary among different fibrocartilages in the same individual. Variations in heterogeneity among different anatomical sites may be attributed to the distinct origins of cartilage cells between craniofacial and truncal tissues. These specific embryonic origins are accompanied by distinct behavior of cartilage progenitor cells.[26] The characterization of the tissue microenvironment in the fibrocartilage in which CD90$^+$ cells reside in 7-day-old mice may provide valuable insights into these differences and a possible explanation for the low stemness of CD90$^+$ cells from TMJ disc.

The CD90$^+$ cell expression was mainly located in the anterior band of the TMJ disc, with a few cells that were distributed in the posterior band near the attachment site. This was consistent with previous results from staining the TMJ disc, where CD90 was considered a marker for the mural cells in the TMJ disc, which expressed multiple mesenchymal stem cell markers.[21] In the condylar cartilage, the CD90$^+$ cells were mainly located at the fibrous surface layer, where fibrocartilage stem cells with mesenchymal stem cell characteristics have previously been found.[17] In

the meniscus, the CD90$^+$ cells were mainly located in the outer vascular-rich region. In the annulus fibrosus of the IVD, the CD90$^+$ cells were mainly located in the outer annulus fibrosus, which is considered to be the stem cell niche of the IVD[27] as well as the area in which blood vessels penetrate during fetal development.[28] It appeared that the distribution of CD90$^+$ cells was mainly concentrated in vascular-rich areas, which suggests a potential regulating role of the peri-vascular cell niche in fibrocartilage repair and regeneration. Cells, blood vessels, matrix glycoproteins, and the 3-dimensional space formed by this architecture provide a highly specialized microenvironment for stem cells.[29] Blood vessels supply undifferentiated MSCs with nutrients to induce healing,[30] and the presence of growth factors and cytokines in the blood is capable of enhancing tissue regeneration and repair.[31]

There were relatively more CD90$^+$ cells present in the TMJ disc during the early postnatal stage, but only a very few CD90$^+$ cells with active proliferation capacity were found. Though the TMJ disc and condylar cartilage were shown to have a close relationship with the spatial distribution and developmental origin, our data showed that the CD90$^+$ cells in the condylar cartilage and disc cartilage had distinct stem cell features. Indeed, both the TMJ disc and condylar cartilage had few actively proliferating CD90$^+$ cells compared with the meniscus and annulus fibrosus of the IVD, which may be one reason for the restricted capacity for repair of the degeneration of TMJ cartilage.

Our study also suggested that the TMJ disc may have undergone a dramatic metabolic change during the early stages of growth and development. Although all tissues experience a decrease in cell density during early development, the TMJ disc exhibits the most pronounced decrease in cell density. This observation may indicate more extensive tissue remodeling and restructuring than in the other 3 fibrocartilage tissues, which was potentially due to the loss of stem cell capacity in this delicate cartilaginous tissue. Another unique feature of the TMJ disc is that it consistently exhibits low levels of proteoglycans. These molecules help form the hydrated gel-like matrix of fibrocartilage, which gives the tissue its ability to absorb and distribute mechanical forces.[32] This suggests that the TMJ disc is more susceptible to damage under load-bearing conditions.

Several limitations exist in this study. Post-pubertal tissues in females were excluded. Estrogen, as the primary determinant of female gender, exhibits different effects on the TMJ cartilage, knee joint cartilage, and IVD. Estrogen enhances inflammation in TMJ disease,[33,34] which is in contrast to its typical protective role in knee joint cartilage[35] and intervertebral discs,[36] where estrogen is believed to maintain joint homeostasis. Exposure to 17-β estradiol resulted in a substantial reduction of collagen and glycosaminoglycan content in TMJ fibrocartilage, suggesting an early manifestation of degenerative TMJ disorders, whereas no discernible impact was observed on the fibrocartilaginous matrix of the meniscus in the knee joint.[37] Therefore, this study excluded tissues from post-pubertal females when investigating histological cellular density and matrix changes.

Overall, we highlight the spatial heterogeneity of CD90$^+$ cells in the fibrocartilages of different joint tissues and provide evidence for the restricted stem cell characteristics of CD90$^+$ cells in the TMJ disc, which may contribute to its limited cartilage repair capacity. These findings may offer insights into the potential target cell populations in treatments for degenerated TMJ cartilage.

Authors' Note

The work reported was done in State Key Laboratory of Oral Diseases & National Center for Stomatology & National Clinical Research Center for Oral Diseases, Sichuan University.

Acknowledgments and Funding

The author(s) disclosed receipt of the following financial support for the research, authorship, and/or publication of this article: This study was supported by National Natural Science Foundation of China (NSFC) No. 82071139 (to S.Z.), 82270999 (to R.B.); Key R&D Program of Sichuan Provincial Department of Science and Technology No. 23ZDYF2130 (to S.Z.); and 'From Zero to One' Innovative Research Program of Sichuan University No. 2022SCUH0022 (to R.B.).

Declaration of Conflicting Interests

The author(s) declared no potential conflicts of interest with respect to the research, authorship, and/or publication of this article.

ORCID iD

Ruiye Bi https://orcid.org/0000-0002-8297-9691

References

1. Benjamin M, Ralphs JR. Biology of fibrocartilage cells. Int Rev Cytol. 2004;233:1-45. doi:10.1016/s0074-7696(04)33001-9.
2. Huey DJ, Hu JC, Athanasiou KA. Unlike bone, cartilage regeneration remains elusive. Science. 2012;338(6109):917-21. doi:10.1126/science.1222454.
3. Sofat N, Ejindu V, Kiely P. What makes osteoarthritis painful? The evidence for local and central pain processing. Rheumatology (Oxford). 2011;50(12):2157-65. doi:10.1093/rheumatology/ker283.
4. Manfredini D, Guarda-Nardini L, Winocur E, Piccotti F, Ahlberg J, Lobbezoo F. Research diagnostic criteria for temporomandibular disorders: a systematic review of axis I epidemiologic findings. Oral Surg Oral Med Oral Pathol Oral Radiol Endod. 2011;112(4):453-62. doi:10.1016/j.tripleo.2011.04.021.
5. Valesan LF, Da-Cas CD, Réus JC, Denardin ACS, Garanhani RR, Bonotto D, *et al*. Prevalence of temporomandibular

joint disorders: a systematic review and meta-analysis. Clin Oral Investig. 2021;25(2):441-53. doi:10.1007/s00784-020-03710-w.
6. Gee SM, Tennent DJ, Cameron KL, Posner MA. The burden of meniscus injury in young and physically active populations. Clin Sports Med. 2020;39(1):13-27. doi:10.1016/j.csm.2019.08.008.
7. Adams BG, Houston MN, Cameron KL. The epidemiology of meniscus injury. Sports Med Arthrosc Rev. 2021;29(3): e24-33. doi:10.1097/jsa.0000000000000329.
8. Teraguchi M, Yoshimura N, Hashizume H, Muraki S, Yamada H, Minamide A, *et al*. Prevalence and distribution of intervertebral disc degeneration over the entire spine in a population-based cohort: the Wakayama Spine Study. Osteoarthritis Cartilage. 2014;22(1):104-10. doi:10.1016/j.joca.2013.10.019.
9. Francisco V, Pino J, González-Gay MÁ, Lago F, Karppinen J, Tervonen O, *et al*. A new immunometabolic perspective of intervertebral disc degeneration. Nat Rev Rheumatol. 2022;18(1):47-60. doi:10.1038/s41584-021-00713-z.
10. Brinjikji W, Luetmer PH, Comstock B, Bresnahan BW, Chen LE, Deyo RA, *et al*. Systematic literature review of imaging features of spinal degeneration in asymptomatic populations. AJNR Am J Neuroradiol. 2015;36(4):811-6. doi:10.3174/ajnr.A4173.
11. Michelotti A, Rongo R, D'Antò V, Bucci R. Occlusion, orthodontics, and temporomandibular disorders: cutting edge of the current evidence. J World Fed Orthod. 2020;9(3): S15-8. doi:10.1016/j.ejwf.2020.08.003.
12. Marpaung C, van Selms MKA, Lobbezoo F. Temporomandibular joint anterior disc displacement with reduction in a young population: prevalence and risk indicators. Int J Paediatr Dent. 2019;29(1):66-73. doi:10.1111/ipd.12426.
13. Jivnani HM, Tripathi S, Shanker R, Singh BP, Agrawal KK, Singhal R. A study to determine the prevalence of temporomandibular disorders in a young adult population and its association with psychological and functional occlusal parameters. J Prosthodont. 2019;28(1): e445-9. doi:10.1111/jopr.12704.
14. Bielajew BJ, Donahue RP, Espinosa MG, Arzi B, Wang D, Hatcher DC, *et al*. Knee orthopedics as a template for the temporomandibular joint. Cell Rep Med. 2021;2(5):100241. doi:10.1016/j.xcrm.2021.100241.
15. Makris EA, Gomoll AH, Malizos KN, Hu JC, Athanasiou KA. Repair and tissue engineering techniques for articular cartilage. Nat Rev Rheumatol. 2015;11(1):21-34. doi:10.1038/nrrheum.2014.157.
16. Shen W, Chen J, Zhu T, Chen L, Zhang W, Fang Z, *et al*. Intra-articular injection of human meniscus stem/progenitor cells promotes meniscus regeneration and ameliorates osteoarthritis through stromal cell-derived factor-1/CXCR4-mediated homing. Stem Cells Transl Med. 2014;3(3):387-94. doi:10.5966/sctm.2012-0170.
17. Embree MC, Chen M, Pylawka S, Kong D, Iwaoka GM, Kalajzic I, *et al*. Exploiting endogenous fibrocartilage stem cells to regenerate cartilage and repair joint injury. Nat Commun. 2016;7:13073. doi:10.1038/ncomms13073.
18. Brown S, Matta A, Erwin M, Roberts S, Gruber HE, Hanley EN, *et al*. Cell clusters are indicative of stem cell activity in the degenerate intervertebral disc: can their properties be manipulated to improve intrinsic repair of the disc? Stem Cells Dev. 2018;27(3):147-65. doi:10.1089/scd.2017.0213.
19. Saalbach A, Anderegg U. Thy-1: more than a marker for mesenchymal stromal cells. FASEB J. 2019;33(6):6689-96. doi:10.1096/fj.201802224R.
20. Zhang Y, Xu X, Zhou P, Liu Q, Zhang M, Yang H, *et al*. Elder mice exhibit more severe degeneration and milder regeneration in temporomandibular joints subjected to bilateral anterior crossbite. Front Physiol. 2021;12:750468. doi:10.3389/fphys.2021.750468.
21. Bi R, Yin Q, Li H, Yang X, Wang Y, Li Q, *et al*. A single-cell transcriptional atlas reveals resident progenitor cell niche functions in TMJ disc development and injury. Nat Commun. 2023;14(1):830. doi:10.1038/s41467-023-36406-2.
22. Gamer LW, Shi RR, Gendelman A, Mathewson D, Gamer J, Rosen V. Identification and characterization of adult mouse meniscus stem/progenitor cells. Connect Tissue Res. 2017;58(3-4):238-45. doi:10.1080/03008207.2016.1271797.
23. Bi R, Yin Q, Mei J, Chen K, Luo X, Fan Y, *et al*. Identification of human temporomandibular joint fibrocartilage stem cells with distinct chondrogenic capacity. Osteoarthritis Cartilage. 2020;28(6):842-52. doi:10.1016/j.joca.2020.02.835.
24. da Silva Meirelles L, Caplan AI, Nardi NB. In search of the in vivo identity of mesenchymal stem cells. Stem Cells. 2008;26(9):2287-99. doi:10.1634/stemcells.2007-1122.
25. Dominici M, Le Blanc K, Mueller I, Slaper-Cortenbach I, Marini F, Krause D, *et al*. Minimal criteria for defining multipotent mesenchymal stromal cells. The International Society for Cellular Therapy position statement. Cytotherapy. 2006;8(4):315-7. doi:10.1080/14653240600855905.
26. Weber M, Wehrhan F, Deschner J, Sander J, Ries J, Möst T, *et al*. The special developmental biology of craniofacial tissues enables the understanding of oral and maxillofacial physiology and diseases. Int J Mol Sci. 2021;22(3). doi:10.3390/ijms22031315.
27. Lyu FJ, Cheung KM, Zheng Z, Wang H, Sakai D, Leung VY. IVD progenitor cells: a new horizon for understanding disc homeostasis and repair. Nat Rev Rheumatol. 2019;15(2):102-12. doi:10.1038/s41584-018-0154-x.
28. Smith LJ, Elliott DM. Formation of lamellar cross bridges in the annulus fibrosus of the intervertebral disc is a consequence of vascular regression. Matrix Biol. 2011;30(4):267-74. doi:10.1016/j.matbio.2011.03.009.
29. Mohyeldin A, Garzón-Muvdi T, Quiñones-Hinojosa A. Oxygen in stem cell biology: a critical component of the stem cell niche. Cell Stem Cell. 2010;7(2):150-61. doi:10.1016/j.stem.2010.07.007.
30. de Albornoz PM, Forriol F. The meniscal healing process. Muscles Ligaments Tendons J. 2012;2(1):10-8.
31. Schmidt MB, Chen EH, Lynch SE. A review of the effects of insulin-like growth factor and platelet derived growth factor on in vivo cartilage healing and repair. Osteoarthritis Cartilage. 2006;14(5):403-12. doi:10.1016/j.joca.2005.10.011.
32. Moo EK, Ebrahimi M, Sibole SC, Tanska P, Korhonen RK. The intrinsic quality of proteoglycans, but not collagen fibres, degrades in osteoarthritic cartilage. Acta Biomater. 2022;153:178-89. doi:10.1016/j.actbio.2022.09.002.

33. Chen J, Kamiya Y, Polur I, Xu M, Choi T, Kalajzic Z, *et al*. Estrogen via estrogen receptor beta partially inhibits mandibular condylar cartilage growth. Osteoarthritis Cartilage. 2014;22(11):1861-8. doi:10.1016/j.joca.2014.07.003.
34. Wang XD, Kou XX, Meng Z, Bi RY, Liu Y, Zhang JN, *et al*. Estrogen aggravates iodoacetate-induced temporomandibular joint osteoarthritis. J Dent Res. 2013;92(10):918-24. doi:10.1177/0022034513501323.
35. Ma HL, Blanchet TJ, Peluso D, Hopkins B, Morris EA, Glasson SS. Osteoarthritis severity is sex dependent in a surgical mouse model. Osteoarthritis Cartilage. 2007;15(6):695-700. doi:10.1016/j.joca.2006.11.005.
36. Shelby T, Mills ES, Ton A, Wang JC, Hah RJ, Qureshi SA, *et al*. The role of sex hormones in degenerative disc disease. Global Spine J. Epub 2023 Jan 18. doi:10.1177/21925682231152826.
37. Park Y, Chen S, Ahmad N, Hayami T, Kapila S. Estrogen selectively enhances TMJ disc but not knee meniscus matrix loss. J Dent Res. 2019;98(13):1532-8. doi:10.1177/0022034519875956.